

Interference-induced suppression of particle emission from a Bose-Einstein condensate in lattice with time-periodic modulations

L. Q. Lai^{1,*} and Z. Li^{2,†}

¹*School of Science, Nanjing University of Posts and Telecommunications, Nanjing 210023, China*

²*School of Electronic Engineering, Chengdu Technological University, Chengdu 611730, China*

(Dated: January 11, 2024)

Collective emission of particles from a parametrically driven condensate has attracted significant experimental and theoretical attention due to the appealing visual effects and potential metrological applications. In this paper, we investigate the particle emission from a Bose-Einstein condensate confined in a one-dimensional lattice with periodically modulated interparticle interactions. We give the regimes for discrete modes, and find that the emission is distinctly suppressed. The configuration induces a broad band, but due to the interference of the matter waves few particles can be ejected. We further qualitatively model the emission process, and demonstrate the short-time behaviors. This engineering provides a way for manipulating the propagation of particles and the corresponding dynamics of condensates in lattices, and may find use in other nonequilibrium problems with time-periodic driving.

I. INTRODUCTION

The ability of precisely manipulating the interparticle interactions in many-body systems has provided opportunities of investigating the exotic behaviors of quantum matters and controlling the quantum engineering [1], as well as demonstrating a variety of fundamental physical problems, such as quantum phase transition and nonequilibrium dynamics [2]. Time-periodic driving is one of the major schemes especially implemented in experiments, which opens possibilities of the explorations on fascinating quantum phenomena [3, 4] and the remarkable applications in a large class of platforms, ranging from topological systems [5–8] to optical lattices [9–12].

Coherent manipulation is particularly promising in the gases of ultracold atoms, where the excitation of atoms from a Bose-Einstein condensate can be well controlled via Feshbach resonances [13, 14]. Pair atoms shared the energy from the periodic drive, and were ejected in opposite directions after collisions, leading to the collective emission of matter-wave jets resembling fireworks [15]. A number of subsequent advances revealing new aspects of Bose fireworks have been reported [16–35], where in the theoretical side lattice models were introduced as a transparent way of studying the relevant physics. The behavior of the trapped atoms was mimicked by the hopping of particles from the condensate to the leads and between neighboring sites. In addition to the experimentally observed pair emission, a novel single-particle emission [32], the resonant enhancement [33], the effects of drive imbalance [34], as well as a distinctly intermittent emission [35] have been demonstrated, respectively.

In cold atom experiments, one can not only configure unconventional lattice structures to reveal novel nonequilibrium effects, but also control the couplings of

the lattices based on special requirements, where the properties of the particles would be probably varied. Most of the previous works paid attention to the stimulated excitations and the resulting particle jets, while it would be also conducive to move along the opposite direction, i.e., the possible suppression of the collective emission. In Ref. [33] we focused on a periodically driven condensate in a one-dimensional lattice to demonstrate the parametric resonance, where a local deep trap confined two central sites, with each site solely connected to the left or right lead. Here we introduce a similar geometry, however, with some more sophisticated setups, where the central sites are coupled to both leads. We analyze the dynamics within perturbative analysis and figure out the available broad band for discrete modes. When compared with the previous results, we find the strong suppression of particle emission from the trap, and present both analytical and numerical calculations to qualitatively model the short-time process.

The paper is organized as follows. In Sec. II we illustrate our theoretical model and the corresponding equations of motion, and use perturbative analysis to discuss the regimes of the discrete modes. In Sec. III we compare the solutions from the present work with a previous one to demonstrate the suppression of the particle emission, and further qualitatively clarify the results. A summary is given in Sec. IV.

II. MODEL AND PERTURBATION

The system under consideration is a one-dimensional infinite lattice, as depicted in Fig. 1, where a local trapping potential of depth V is placed to confine a Bose-Einstein condensate. The central sites labeled a and b are coupled with amplitude t_{ab} , which enables the tunnelling of particles from one site to the other. Atoms with sufficient energy can run away from the trap, while hopping onto either site a_1 or b_1 with strength t_c , and

* lqlai@njupt.edu.cn

† leezhao@hnu.edu.cn

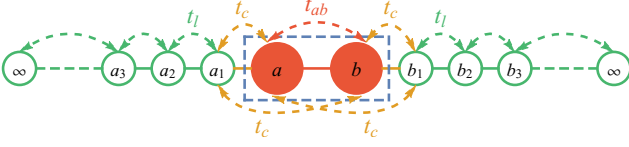


FIG. 1. (color online) Illustration of the one-dimensional geometry. The red solid circles symbolize the central sites in a local deep trap denoted by the blue dashed box, which clarifies the couplings of a and b with a_1 and b_1 . The green empty circles labeled by $a_1(b_1), a_2(b_2), \dots, \infty$ represent the sites on each lead.

the couplings between neighboring sites in each lead are quantified by t_l . The geometric structure can be specifically realized in experiments by putting a condensate in a double-well potential in optical lattices combined with microtraps [36, 37].

For simplicity, we only take the interactions between atoms which sit on the central sites into account, and neglect those outside of the trap. Thus the Hamiltonian of such a system reads

$$\begin{aligned} \hat{H} = & V \left(\hat{a}_0^\dagger \hat{a}_0 + \hat{b}_0^\dagger \hat{b}_0 \right) - t_{ab} \left(\hat{a}_0^\dagger \hat{b}_0 + \hat{b}_0^\dagger \hat{a}_0 \right) \\ & + \frac{1}{2} [U + g(t)] \left(\hat{a}_0^\dagger \hat{a}_0^\dagger \hat{a}_0 \hat{a}_0 + \hat{b}_0^\dagger \hat{b}_0^\dagger \hat{b}_0 \hat{b}_0 \right) \\ & - t_c \left(\hat{a}_1^\dagger \hat{a}_0 + \hat{a}_1^\dagger \hat{b}_0 + \hat{b}_1^\dagger \hat{a}_0 + \hat{b}_1^\dagger \hat{b}_0 + \text{H.c.} \right) \\ & - t_l \sum_{j=1}^{\infty} \left(\hat{a}_{j+1}^\dagger \hat{a}_j + \hat{b}_{j+1}^\dagger \hat{b}_j + \text{H.c.} \right), \end{aligned} \quad (1)$$

where \hat{a}_j^\dagger and \hat{b}_j^\dagger are the creation bosonic operators on the j th site, while \hat{a}_0^\dagger and \hat{b}_0^\dagger correspond to the central sites. A time-independent on-site interaction U and a time-dependent periodic driving $g(t)$ characterize the pairwise particle interactions, for which we take the sinusoidal modulation $g(t) = g \sin(\omega t)$ with g the drive strength and ω the drive frequency.

The lattice involves the nature of a macroscopic number of particles, and hence we can use a mean-field approximation to replace the operators \hat{a} and \hat{b} with some complex numbers a and b , i.e., the absolute squares of the expectation values $a_j = \langle \hat{a}_j \rangle$ and $b_j = \langle \hat{b}_j \rangle$ represent the population of atoms on site j in each lead.

Since the finite U hardly changes the relevant physics [32], by neglecting the on-site interaction term and taking units where $\hbar = 1$, and according to the equations of motion $\partial_t \hat{A} = i[\hat{H}, \hat{A}]$ in the Heisenberg picture, we thus write down, respectively, for the central sites

$$i\partial_t \begin{pmatrix} a_0 \\ b_0 \end{pmatrix} = \begin{pmatrix} \Lambda_a & 0 \\ 0 & \Lambda_b \end{pmatrix} \begin{pmatrix} a_0 \\ b_0 \end{pmatrix} - t_{ab} \begin{pmatrix} b_0 \\ a_0 \end{pmatrix} - t_c \Omega_m \begin{pmatrix} a_0 \\ b_0 \end{pmatrix} \quad (2)$$

with $\Lambda_a = V + g(t)|a_0|^2$, $\Lambda_b = V + g(t)|b_0|^2$ and $\Omega_m =$

$\frac{a_m + b_m}{a_m + b_m}$, and for the sites where $j \geq 1$,

$$i\partial_t \begin{pmatrix} a_1 \\ b_1 \end{pmatrix} = -t_c \Omega_0 - t_l \begin{pmatrix} a_2 \\ b_2 \end{pmatrix}, \quad (3)$$

$$i\partial_t \begin{pmatrix} a_j \\ b_j \end{pmatrix} = -t_l \begin{pmatrix} a_{j+1} \\ b_{j+1} \end{pmatrix} - t_l \begin{pmatrix} a_{j-1} \\ b_{j-1} \end{pmatrix}. \quad (4)$$

At time $t < 0$, the system is in its equilibrium when the drive is absent. We find the stationary solutions by making the ansatz $a_0(t) = \alpha e^{-i\nu t}$, $b_0(t) = \beta e^{-i\nu t}$, where α and β are constant, and assuming that

$$a_1(t) = \frac{\alpha + \beta}{2} e^{-i\nu t} e^{-\lambda_1}, \quad a_2(t) = \frac{\alpha + \beta}{2} e^{-i\nu t} e^{-\lambda_1 - \lambda}. \quad (5)$$

The linear Eq. (4) leads to $a_j/a_{j-1} = b_j/b_{j-1} = e^{-\lambda}$, thus $\cosh \lambda = \nu/(-2t_l)$, and for $j \geq 1$ we have explicitly

$$a_j(t) = b_j(t) = \frac{\alpha + \beta}{2} e^{-i\nu t} e^{-\lambda_1} e^{-\lambda(j-1)} \quad (6)$$

with $\lambda_1 = -\ln[-2t_c/(\nu + t_l e^{-\lambda})]$. Eliminating the leads based on the Green's function technique [33]

$$a_j(t) = b_j(t) = -t_c \int^t d\tau G_{j1}(t - \tau) [a_0(\tau) + b_0(\tau)] \quad (7)$$

where $G_{j1}(t) = i^{j-2} [j J_j(2t_l t)] \theta(t) / (t_l t)$ is the time-domain Green's function with $J_n(x)$ the Bessel function of the first kind and $\theta(t)$ the step function, we obtain the nonlinear integro-differential equation

$$\begin{aligned} i\partial_t \begin{pmatrix} a_0 \\ b_0 \end{pmatrix} = & \begin{pmatrix} \Lambda_a & 0 \\ 0 & \Lambda_b \end{pmatrix} \begin{pmatrix} a_0 \\ b_0 \end{pmatrix} - t_{ab} \begin{pmatrix} b_0 \\ a_0 \end{pmatrix} \\ & + 2t_c^2 \int^t G_{11}(t - \tau) d\tau \Omega_0(\tau). \end{aligned} \quad (8)$$

To largely simplify the analysis, we treat g as a small parameter, where one could begin by finding the perturbative solution with $g = 0$. Through this Eq. (8) becomes a linear equation, whose solutions are linear combinations of functions of a_0 and b_0 , with

$$\nu \alpha = V \alpha - t_{ab} \beta + 2t_c^2 G_{11}(\nu) (\alpha + \beta), \quad (9)$$

$$\nu \beta = V \beta - t_{ab} \alpha + 2t_c^2 G_{11}(\nu) (\alpha + \beta), \quad (10)$$

where, as in Ref. [32], the frequency-domain Green's function reads

$$G_{11}(\epsilon) = \frac{\epsilon}{2t_l^2} - i \sqrt{\frac{1}{t_l^2} - \frac{\epsilon^2}{4t_l^4}}. \quad (11)$$

We want the symmetric mode with $\beta = \alpha$ to be stable, which means that there should be a real-valued solution to the equation

$$\nu - V + t_{ab} - 4t_c^2 G_{11}(\nu) = 0, \quad (12)$$

and it specifically constrains the allowed values of the trapping potential V . While the above equation can be

readily solved by substituting in the expression for G_{11} and shuffling terms around, it suffices for us to perturbatively solve it. To the zeroth order in t_c , we obtain an explicit expression

$$\nu_s^{(0)} = V - t_{ab}, \quad (13)$$

while at the second order one simply substitutes this into Eq. (12) to get

$$\nu_s^{(2)} = V - t_{ab} + \frac{2t_c^2}{t_l^2} \left(V - t_{ab} - i\sqrt{4t_l^2 - (V - t_{ab})^2} \right), \quad (14)$$

which leads to the constraints of $|V - t_{ab}| > 2t_l$. Specializing to the case where $V = -|V| < 0$, in the symmetric mode we subsequently reach the allowed values of the trapping potential as $|V| + t_{ab} > 2t_l$.

One can also, in this slick way, obtain the frequency of the antisymmetric mode $\beta = -\alpha$ for both the zeroth and the second order of t_c , with

$$\nu_a^{(0)} = \nu_a^{(2)} = V + t_{ab}. \quad (15)$$

To observe significant particle emission, we need to parametrically excite the antisymmetric mode, which requires the complex solutions. However, under this circumstance they have explicitly only real values in both orders. As a consequence, we are probably incapable of being in the regime where the symmetric mode is stable but the antisymmetric mode is damped, i.e., the collective emission of particles could be greatly suppressed, and there exists merely a very weak jet.

III. PARAMETRIC DRIVE

For the verification of the scenario, we now parametrically drive the system and explore its nonlinear dynamics by numerically solving Eq. (8). We assume that the weak drive is turned on at time $t = 0$. We introduce, without any loss of generality, initially slight difference for $a_0(t = 0) = \alpha = 1.01$ and $b_0(t = 0) = \beta = 1$ to seed the system at the lowest symmetric mode of $\nu_s = V - t_{ab}$. We also fix $t_{ab} = 1$ as the energy scale of the system in most of the numerics, such that the times are measured in units of \hbar/t_{ab} .

We first compare the collective emission of particles in the present model with the previous one from Ref. [33], by showing their decaying behaviors under typical drive frequencies. Specifically they are both two-site infinite lattices, but the previous one exhibited a resonant enhancement. As can be plainly seen in Fig. 2, when the drive strength is as small as $g = 0.1$ and the drive frequency is $\omega = 4t_{ab}$, for the previous model the number of trapped atoms $N = |a_0|^2 + |b_0|^2$ bears a short plateau around $t < 100$ with only a few particles escaped. At intermediate times $150 < t < 250$ the condensate suddenly starts to eject a burst of atoms, until that few are

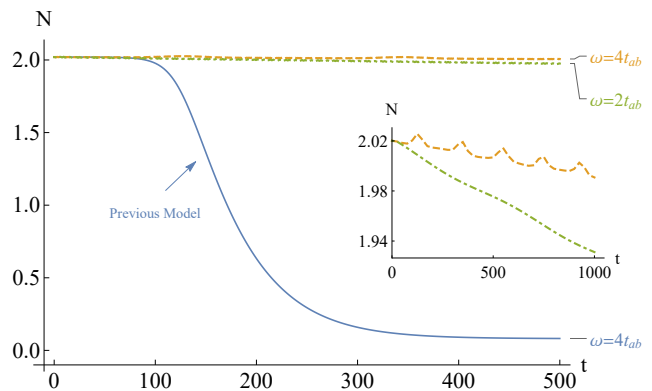


FIG. 2. (color online) Time dependence of the number of trapped atoms N for both models with typical drive frequencies ω . The blue solid line corresponds to the previous two-site model from Ref. [33] with $\omega = 4t_{ab}$, while the green dot-dashed line and the orange dashed line are for the present model with $\omega = 2t_{ab}$ and $\omega = 4t_{ab}$, respectively. Inset shows a more detailed behavior of the present model with a longer time interval. Here, we have kept the drive strength as $g = 0.1$ and the trapping potential as $V = -2$. The coupling strengths are $t_c = 0.1$ and $t_l = 1$. Energies are in units of t_{ab} , and times are in units of \hbar/t_{ab} .

remained. Although they have somewhat similar configurations, the present system undergoes a slow but very steady decay under both frequencies of $\omega = 2t_{ab}$ and $\omega = 4t_{ab}$. The detailed behaviors are characterized in the inset, where a fairly small portion of particles are ejected even in a much longer time interval.

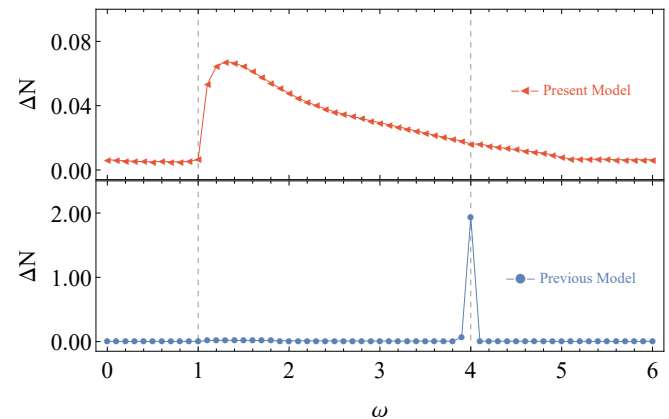


FIG. 3. (color online) Number of excited atoms ΔN under different frequency ω , which is calculated from $\Delta N = (|a_0(t = 0)|^2 + |b_0(t = 0)|^2) - (|a_0(t = t_e)|^2 + |b_0(t = t_e)|^2)$, up to time $t_e = 500$. The upper panel corresponds to the present model, while the lower panel comes from the previous model in Ref. [33]. The trapping potential is $V = -2$, and the drive strength is $g = 0.1$. The coupling strengths are $t_c = 0.1$ and $t_l = 1$. Energies are in units of t_{ab} , and times are in units of \hbar/t_{ab} .

To check that whether the discrepancies shown above

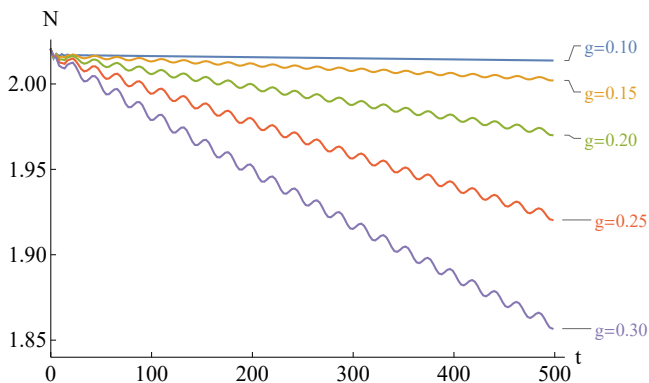


FIG. 4. (color online) Time dependence of the number of trapped atoms N for the present model with different drive strength g . Here, the drive frequency is fixed as $\omega = 2t_{ab}$, and we have taken $V = -2$, $t_c = 0.1$ and $t_l = 1$. Energies are in units of t_{ab} , and times are in units of \hbar/t_{ab} .

are induced by the selection of certain drive frequencies, in Fig. 3 we keep the drive strength as $g = 0.1$ while sweeping the frequency, and also compare the corresponding results from Ref. [33]. For the previous model, a distinct peak appears at $\omega = 4t_{ab}$ with a typical narrow bandwidth, while for other non-resonant frequencies there are hardly ejected atoms. In contrast, a broader band emerges roughly from $\omega = t_{ab}$ to $\omega = 4t_{ab}$ for the present model, with very few excited atoms. Even when we tune to a relatively larger drive strength (e.g. $g = 0.3$), as shown in Fig. 4, the number N can oscillate and fall with a greater extent, but there seems to be still a small particle jet rather than large pulse, which indicates that with such a configuration the collective emission is distinctly suppressed.

For the two-site lattice in the previous model, once the periodic modulation is turned on, the condensate wave functions undergo oscillations and the atoms in the ground state are subsequently pumped to a higher energy level corresponding to the antisymmetric mode. The excited atoms with sufficient energy escape from the trap and travel along the leads to form the jets, exhibiting a parametric resonance. With respect to the present configuration, the main difference from the previous model exists in Eq. (7), where two branches of the matter waves coming from sites a and b tunnel and interfere due to the sophisticated hoppings, where the decay rate of the particles is far inferior to the growth rate, resulting in that the antisymmetric mode can hardly leak into the lead, and there are no longer significant particle jets.

To demonstrate the formalism, in the limit where t_c is negligible we qualitatively model the process with the help of the method of multiple scales, where

$$a_0(t) = e^{-i\nu_s t} u(t) + e^{-i\nu_a t} v(t), \quad (16)$$

$$b_0(t) = e^{-i\nu_s t} u(t) - e^{-i\nu_a t} v(t), \quad (17)$$

with $u(t)$ and $v(t)$ both slowly varying, and $\nu_{(s,a)}$ the zeroth-order frequencies corresponding to the discrete

modes. Substituting the ansatz into Eq. (8) and collecting the terms leads to (see Appendix A)

$$\partial_t u = 2gX(t)v^2 u, \quad (18)$$

$$\partial_t v = -2gX(t)u^2 v, \quad (19)$$

where $X(t) = \sin(\omega t) \sin(4t_{ab} t)$. Since u^2 represents the number of particles in the symmetric mode, and v^2 corresponds to that in the antisymmetric mode, if one linearizes about $v = 0$, i.e., all particles are initially placed in the ground state, from the above equations we find v decays to zero while u grows. In other words, we are not able to produce large particle jets by leaking the antisymmetric mode into the lead.

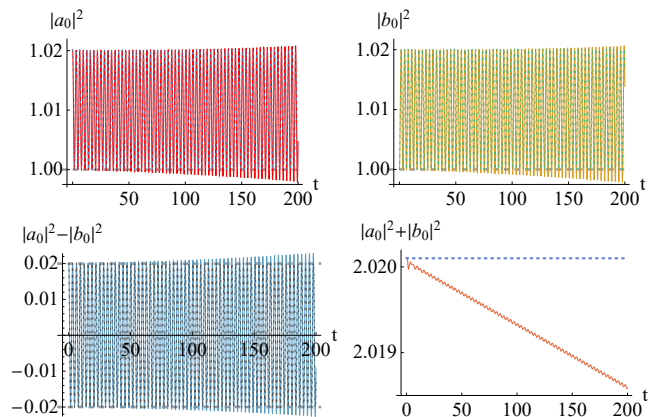


FIG. 5. (color online) Typical examples of the time evolution of the particle number $|a_0|^2$ and $|b_0|^2$ on both central sites, the imbalance $|a_0|^2 - |b_0|^2$ and the total particle number in the condensate $|a_0|^2 + |b_0|^2$. The analytical solutions (dotted line) and the numerical results (solid line) are nearly indistinguishable at short times. Here, the drive strength is $g = 0.1$, the drive frequency is fixed as $\omega = 2t_{ab}$ and the coupling strength is tuned to $t_c = 0.01$. We have also taken $V = -2$ and $t_l = 1$. Energies are in units of t_{ab} , and times are in units of \hbar/t_{ab} .

Figure 5 compares the analytical solutions coming from Eqs. (18) and (19) with the numerical results, when the coupling strength is tuned to $t_c = 0.01$. Both outcomes clearly describe the rapid oscillation and slow time evolution of the short-time behavior of the system, and they fit quite well at rough times $t < 80$. For longer intervals, the deviations emerge, where the numerics show that the particle imbalance $|a_0|^2 - |b_0|^2$ oscillates around and grows up with time rather than falls, under which the system maintains in the stage of build-up, corresponding to the fact that the total particle number $|a_0|^2 + |b_0|^2$ from the numerics drops very slightly.

There can always be certain oscillations and ejected particles from the condensate once the driving field is applied, while the analytical formalism, which is limited in the regime where the drive strength g and the coupling strength t_c are both negligible, demonstrates the approximate stability throughout. Therefore, for a larger drive the linearization is no longer justified. We further illustrate the structure of a jet by plotting the number of

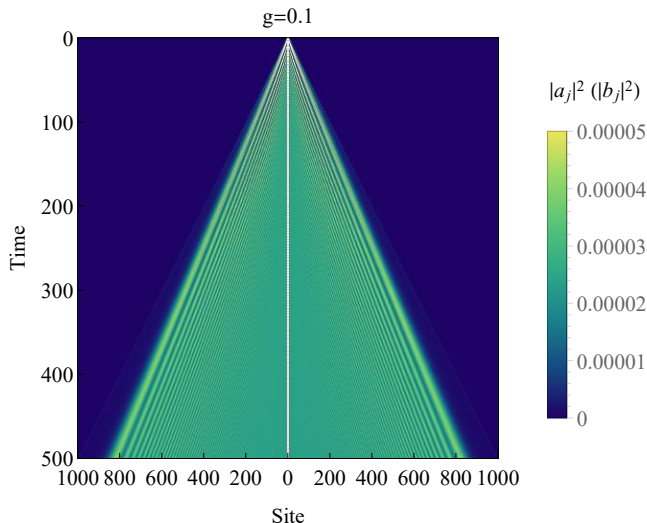


FIG. 6. (color online) Number of the particles on the j th site of each lead as a function of time. Here, we have taken $V = -2$, $g = 0.1$, $\omega = 2t_{ab}$, $t_c = 0.1$ and $t_l = 1$. Energies are in units of t_{ab} , and times are in units of \hbar/t_{ab} . Note the scaled legend.

particles on each site of the leads, as shown in Fig. 6. The pulses can be moderately visible here, with fairly few ejected particles.

IV. SUMMARY

We have introduced a one-dimensional lattice, where the trapped central sites are coupled with both leads, to investigate the collective emission of particles from a Bose-Einstein condensate with time-periodic modulations. Perturbative analysis is used for simplification, for which we validate through numerical calculations.

In a previous work where the configuration was somewhat similar, the collective modes resulted in a dramatic enhancement such that a small drive could induce large pulses when the drive frequency was tuned to resonance [33]. In the present model, however, the couplings give rise to a broader band, with only few particles ejected even when the drive strengths are increased, i.e., the emission is greatly suppressed. Since the central sites are coupled with both leads, this phenomenon might be attributed to the interference of the outgoing matter waves from the central sites, where the decay rate of the particles is much lower than the growth rate, leading to insignificant particle jets outside of the trap.

The geometries and the couplings can be readily implemented with optical lattices in experiments. One could, based on particular purposes, utilize specific engineering to either enhance or suppress the emission processes, and such framework would enable an intensive study of the correlations among the particle emission, the couplings and the various leads.

ACKNOWLEDGEMENTS

L.Q.L would like to thank Professor Erich J. Mueller for the profound instructions. This work was supported by the Natural Science Research Start-up Foundation of Recruiting Talents of Nanjing University of Posts and Telecommunications (Grant No. NY223065), the China Scholarship Council (Grant No. 201906130092), and Natural Foundation of Sichuan Province (Grant No. 2023NSFSC1330).

Appendix A: Derivation of the analytical relation

Here we utilize the method of multiple scales to reproduce the results from Sec. III, in the limit where the drive strength g and the coupling strength t_c are small. Substituting Eqs. (16) and (17) into Eq. (8), and neglecting the slow variation of any function $f(t)$ in the integral by

$$\int^t G_{11}(t-\tau)f(\tau)e^{-i\xi\tau}d\tau \approx f(t)e^{-i\xi t}G_{11}(\xi), \quad (\text{A1})$$

as well as using the neat combinations

$$g \sin(\omega t)(|a_0|^2 a_0 + |b_0|^2 b_0) = \frac{g}{i} (e^{i\omega t} - e^{-i\omega t}) \times (e^{-i\nu_s t}(|u|^2 + 2|v|^2)u + e^{i(\nu_s - 2\nu_a)t}v^2 u^*), \quad (\text{A2})$$

$$g \sin(\omega t)(|a_0|^2 a_0 - |b_0|^2 b_0) = \frac{g}{i} (e^{i\omega t} - e^{-i\omega t}) \times (e^{-i\nu_a t}(2|u|^2 + |v|^2)v + e^{i(\nu_a - 2\nu_s)t}u^2 v^*), \quad (\text{A3})$$

we thus write down the equations of motion for u and v ,

$$\begin{aligned} i\partial_t \frac{a_0 + b_0}{2} &= (\nu_s u + i\partial_t u)e^{-i\nu_s t} \\ &= (V - t_{ab})ue^{-i\nu_s t} + \frac{g \sin(\omega t)}{2}(|a_0|^2 a_0 + |b_0|^2 b_0) \\ &\quad + 2t_c^2 \int^t G_{11}(t-\tau)e^{-i\nu_s \tau}u(\tau), \end{aligned} \quad (\text{A4})$$

$$\begin{aligned} i\partial_t \frac{a_0 - b_0}{2} &= (\nu_a v + i\partial_t v)e^{-i\nu_a t} \\ &= (V + t_{ab})ve^{-i\nu_a t} + \frac{g \sin(\omega t)}{2}(|a_0|^2 a_0 - |b_0|^2 b_0), \end{aligned} \quad (\text{A5})$$

which can be transformed into

$$\begin{aligned} \partial_t u &= -2it_c^2 G_{11}(\nu_s)u - \frac{g}{2} [e^{i\omega t}(|u|^2 + 2|v|^2)u \\ &\quad + e^{i(\omega + 2\nu_s - 2\nu_a)t}v^2 u^* - e^{-i\omega t}(2|u|^2 + |v|^2)v \\ &\quad - e^{i(\omega + 2\nu_a - 2\nu_s)t}u^2 v^*], \end{aligned} \quad (\text{A6})$$

$$\begin{aligned} \partial_t v &= -\frac{g}{2} [e^{i\omega t}(2|u|^2 + |v|^2)v + e^{i(\omega + 2\nu_a - 2\nu_s)t}u^2 v^* \\ &\quad - e^{-i\omega t}(2|u|^2 + |v|^2)v - e^{-i(\omega + 2\nu_s - 2\nu_a)t}u^2 v^*] \end{aligned} \quad (\text{A7})$$

Through $u^* \times \text{Eq. (A6)} + u \times \text{Eq. (A6)}^*$ and $v^* \times \text{Eq. (A7)} + v \times \text{Eq. (A7)}^*$, we further obtain

$$\begin{aligned} \partial_t |u|^2 &= \Gamma |u|^2 - \frac{g}{2} \left[e^{i(\omega+2\nu_s-2\nu_a)t} v^2 u^{*2} \right. \\ &\quad + e^{-i(\omega+2\nu_s-2\nu_a)t} v^2 |u|^2 - e^{i(\omega+2\nu_a-2\nu_s)t} v^2 |u|^2 \\ &\quad \left. - e^{-i(\omega+2\nu_a-2\nu_s)t} v^2 u^{*2} \right], \end{aligned} \quad (\text{A8})$$

$$\begin{aligned} \partial_t |v|^2 &= -\frac{g}{2} \left[e^{i(\omega+2\nu_a-2\nu_s)t} u^2 v^{*2} + e^{-i(\omega+2\nu_a-2\nu_s)t} u^{*2} v^2 \right. \\ &\quad \left. - e^{i(\omega+2\nu_s-2\nu_a)t} u^{*2} v^2 - e^{-i(\omega+2\nu_s-2\nu_a)t} u^2 v^{*2} \right], \end{aligned} \quad (\text{A9})$$

with $\Gamma = 4t_c^2 \text{Im}G_{11}(\nu_s)$. A nice simplifying assumption is to treat u and v as real, we find

$$\partial_t u = 2gX(t)v^2u, \quad (\text{A10})$$

$$\partial_t v = -2gX(t)u^2v, \quad (\text{A11})$$

where $X(t) = \sin(\omega t) \sin(4t_{ab}t)$. The above equations can readily be numerically solved. Conversely, one could also rewritten from Eqs. (16) and (17) that

$$ue^{-i\nu_s t} = \frac{a_0 + b_0}{2}, \quad (\text{A12})$$

$$ve^{-i\nu_a t} = \frac{a_0 - b_0}{2}, \quad (\text{A13})$$

which can be reconstructed to obtain the particle imbalance

$$\begin{aligned} |a_0|^2 - |b_0|^2 &= 2 \left[uv^* e^{-i(\nu_a - \nu_s)t} + u^* v e^{i(\nu_a - \nu_s)t} \right] \\ &= 4uv \cos(2t_{ab}t), \end{aligned} \quad (\text{A14})$$

and the number of total particles

$$|a_0|^2 + |b_0|^2 = 2(|u|^2 + |v|^2). \quad (\text{A15})$$

-
- [1] I. Bloch, J. Dalibard, and W. Zwerger, *Rev. Mod. Phys.* **80**, 885 (2008).
- [2] A. Polkovnikov, K. Sengupta, A. Silva, and M. Vengalattore, *Rev. Mod. Phys.* **83**, 863 (2011).
- [3] G. Moon, M. S. Heo, Y. Kim, H. R. Noh, and W. Jhe, *Phys. Rep.* **698**, 1 (2017).
- [4] A. Eckardt, *Rev. Mod. Phys.* **89**, 011004 (2017).
- [5] T. Kitagawa, E. Berg, M. Rudner, and E. Demler, *Phys. Rev. B* **82**, 235114 (2010).
- [6] Y. H. Wang, H. Steinberg, P. Jarillo-Herrero, and N. Gedik, *Science* **342**, 453 (2013).
- [7] L. Lu, J. D. Joannopoulos, and M. Soljačić, *Nat. Photon.* **8**, 821 (2014).
- [8] P. Mognini, R. Chitra, and W. Chen, *Europhys. Lett.* **128**, 36001 (2019).
- [9] N. Goldman and J. Dalibard, *Phys. Rev. X* **4**, 031027 (2014).
- [10] C. Schweizer, F. Grusdt, M. Berngruber, L. Barbiero, E. Demler, N. Goldman, I. Bloch, and M. Aidelsburger, *Nat. Phys.* **15**, 1168 (2019).
- [11] K. Wintersperger, M. Bukov, J. Näger, S. Lellouch, E. Demler, U. Schneider, I. Bloch, N. Goldman, and M. Aidelsburger, *Phys. Rev. X* **10**, 011030 (2020).
- [12] B. Song, S. Dutta, S. Bhave, J.-C. Yu, E. Carter, N. Cooper, and U. Schneider, *Nat. Phys.* **18**, 259 (2022).
- [13] S. E. Pollack, D. Dries, R. G. Hulet, K. M. F. Magalhães, E. A. L. Henn, E. R. F. Ramos, M. A. Caracanhas, and V. S. Bagnato, *Phys. Rev. A* **81**, 053627 (2010).
- [14] C. Chin, P. Julienne, and E. Tiesinga, *Rev. Mod. Phys.* **82**, 1225 (2010).
- [15] L. W. Clark, A. Gaj, L. Feng, and C. Chin, *Nature* **551**, 356 (2017).
- [16] H. Fu, L. Feng, B. M. Anderson, L. W. Clark, J. Hu, J. W. Andrade, C. Chin, and K. Levin, *Phys. Rev. Lett.* **121**, 243001 (2018).
- [17] Z. Zhang, K. X. Yao, L. Feng, J. Hu, and C. Chin, *Nat. Phys.* **16**, 652 (2020).
- [18] L. Feng, J. Hu, L. W. Clark, and C. Chin, *Science* **363**, 521 (2019).
- [19] H. Fu, Z. Zhang, K. X. Yao, L. Feng, J. Yoo, L. W. Clark, K. Levin, and C. Chin, *Phys. Rev. Lett.*, **125**, 183003 (2020).
- [20] T. Mežnaršič, R. Žitko, T. Arh, K. Gosar, E. Zupanič, and P. Jeglič, *Phys. Rev. A* **101**, 031601 (2020).
- [21] K. Kim, J. Hur, S. J. Huh, S. Choi, and J.-y. Choi, *Phys. Rev. Lett.* **127**, 043401 (2021).
- [22] T. Chen and B. Yan, *Phys. Rev. A* **98**, 063615 (2018).
- [23] Z. G. Wu and H. Zhai, *Phys. Rev. A* **99**, 063624 (2019).
- [24] L. Y. Chih and M. Holland, *New J. Phys.* **22**, 033010 (2020).
- [25] S. Lellouch and N. Goldman, *Quantum Sci. Technol.* **3**, 024011 (2018).
- [26] G. I. Martone, P.-É. Larré, A. Fabbri, and N. Pavloff, *Phys. Rev. A*, **98**, 063617 (2018).
- [27] P. F. Zhang and Y. F. Gu, *SciPost Phys.* **9**, 079 (2020).
- [28] P. Xu and W. X. Zhang, *Phys. Rev. A* **104**, 023324 (2021).
- [29] N. Liu and Z. C. Tu, *Commun. Theor. Phys.* **72**, 125501 (2020).
- [30] Y. T. Cheng and Z.-Y. Shi, *Phys. Rev. A* **104**, 023307 (2021).
- [31] Y.-Y. Chen, P. F. Zhang, W. Zheng, Z. G. Wu, and H. Zhai, *Phys. Rev. A* **102**, 011301(R) (2020).
- [32] L. Q. Lai, Y. B. Yu, and E. J. Mueller, *Phys. Rev. A* **104**, 033308 (2021).
- [33] L. Q. Lai, Y. B. Yu, and E. J. Mueller, *Phys. Rev. A* **106**, 033302 (2022).
- [34] L. Q. Lai and Z. Li, *Chin. Phys. B* (To appear, DOI: 10.1088/1674-1056/ad1172).
- [35] L. Q. Lai, Z. Li, Q. H. Liu, and Y. B. Yu, *Ann. Phys. (Berlin)* **536**, 2300365 (2024).
- [36] H. Lignier, C. Sias, D. Ciampini, Y. Singh, A. Zenesini, O. Morsch, and E. Arimondo, *Phys. Rev. Lett.* **99**, 220403 (2007).
- [37] S. Kuhr, *Nat. Sci. Rev.* **3**, 170 (2016).